Hydrothermal Synthesis and Structural Characterization of the $(C_nH_{2n+6}N_2)[Mn_3(HPO_3)_4]$ ($n = 3-8$) New Layered Inorganic−Organic Hybrid Manganese(II) Phosphites. Crystal Structure and Spectroscopic and Magnetic Properties of $(C_3H_{12}N_2)[Mn_3(HPO_3)_4]$

Sergio Fernández,[†] José L. Pizarro,[‡] José L. Mesa,[†] Luis Lezama,[†] María I. Arriortua,[‡] Roger Olazcuaga,[#] and Teófilo Rojo*,[†]

Departamento de Química Inorgánica and Departamento de Mineralogía-Petrología, Facultad de Ciencias, Universidad del País Vasco, Apdo. 644, E-48080 Bilbao, Spain, and Institut de Chimie de la Matière Condensée de Bordeaux, 33608 Pessac, France

Received February 8, 2001

The $(C_nH_{2n+6}N_2)[Mn_3(HPO_3)_4]$ ($n = 3-8$) compounds have been prepared by hydrothermal synthesis and characterized by X-ray diffraction data and spectroscopic techniques. The crystal structure of $(C_3H_{12}N_2)[Mn_3(HPO_3)_4]$ has been solved from single-crystal X-ray diffraction. The unit-cell parameters are $a = 9.502(1)$, $b = 5.472(1)$, $c = 14.523(4)$ Å, $\beta = 95.01(3)°$, monoclinic, $C2/m$, with $Z = 2$. The compound shows a layered structure stacked along the *c*-axis with the alkyldiammonium cations placed in the interlayer space. The sheets are formed by Mn_3O_{12} trimer units extended in the *ab*-plane and connected by $(HPO_3)^{2-}$ anions. The study of the $(C_nH_{2n+6}N_2)[Mn_3(HPO_3)_4]$ ($n = 4-8$) phases by X-ray powder diffraction indicates an isotype relation with the propanediammonium compound. The Dq and Racah parameters calculated for $(C_3H_{12}N_2)[Mn_3(HPO_3)_4]$ are Dq = 880, $B = 660$ and $C = 3610$ cm^{-1}. The ESR spectra show isotropic signals with a g-value of 2.008. Magnetic measurements indicate the presence of antiferromagnetic interactions inside the $[Mn_3(HPO_3)_4]^{2-}$ sheets. The J/K value has been estimated to be −15 K by considering that the system behaves like an isolated trimer at high temperatures.

Introduction

The types of microporous materials, tetrahedral- and mixed-framework compounds, with open structures continue to expand in terms of framework-forming elements.[1] The most studied and also largest classes of tetrahedral-framework compounds are aluminosilicates[2]and aluminophosphates,[3] as well as their isomorphic substituted forms. Attempts to synthesize frameworks with elements other than Al, Si, and P, especially with transition metals, have resulted in many new classes, such as gallophosphates,[4] titanosilicates,[5] beryllium,[6] zinc,[7] cobalt,[8] iron,[9,10] vanadium,[11] nickel,[12] and molybdenum phosphates.[13]

Microporous materials containing transition metal elements are a focus of comtemporary research [1,14] due to their novel potential catalytic, electrical, optical, and magnetic properties which are not accessible to the main group systems of tetrahedral framework zeolites. Furthermore, compared with tetrahedral elements in zeolitic aluminum silicates (or phosphates), divalent transition metals have a more coordination flexibility and a stronger tendency to form edge-sharing linkages of metal−oxygen polyhedra. These properties usually lead to difficulties in mimicking a zeolite-type structure, but can lead to the possibility of yielding novel framework structures built from a combination of various metal−oxygen polyhedra. Among these materials, the organically templated iron-phosphates occupy a major position. A number of works dealing with this system has evidenced a considerable structural and compositional diversity.[9,15−20] In this way, three-dimensional, layered structure or isolated single chains are known.[10] The magnetic and spectroscopic properties of some of these phases have been studied.[16,19] Recently, open framework cobalt(II), nickel(II), and manganese(II) phosphates have been prepared and their properties reported.[8,12,21−25]

The structural chemistry of phosphite with elements of the first transition series reveals complex two-dimensional and three-dimensional phases.[26] However, organically templated metal-

* To whom all correspondence should be addressed. E-mail: qiproapt@lg.ehu.es.
[†] Departamento de Química Inorgánica, Universidad del País Vasco.
[‡] Departamento de Mineralogía-Petrología, Universidad del País Vasco.
[#] Institut de Chimie de la Matière Condensée de Bordeaux.

(1) Cheetham, A. K.; Ferey, G.; Loiseau, T. *Angew. Chem., Int. Ed.* **1999**, *38*, 3268.
(2) (a) Barrer, R. M. *Hydrothermal Chemistry of Zeolites*; Academic Press: New York, 1989. (b) Meier, W. M.; Olson, D. H. *Atlas of Zeolite Structure Types*; Elsevier: London, 1996.
(3) Wilson, S. T.; Lok, B. M.; Messina, C. A.; Cannon, T. R.; Flanigen, E. M. *J. Am. Chem. Soc.* **1982**, *104*, 6.
(4) (a) Parise, J. B. *Inorg. Chem.* **1985**, *24*, 4312. (b) Ferey, G. *J. Fluorine Chem.* **1995**, *72*, 187.
(5) Chapman, D. M.; Rol, A. L. *Zeolites* **1990**, *10*, 730.
(6) Gier, T. E.; Stucky, G. D. *Nature* **1991**, *349*, 508.
(7) Yang, G. Y.; Sevov, S. C. *J. Am. Chem. Soc.* **1999**, *121*, 8389.
(8) Feng, P.; Bu, X.; Stucky, G. D. *Nature* **1997**, *388*, 735.
(9) Cavellec, M.; Riou, D.; Ninclaus, C.; Greneche, J. M.; Ferey, G. *Zeolites* **1996**, *17*, 260.
(10) Lii, K.-H.; Huang, Y.-F.; Zima, V.; Huang, C.-Y.; Lin, H.-M.; Jiang, Y.-C.; Liao, F.-L.; Wang, S.-L. *Chem. Mater.* **1998**, *10*, 2599.
(11) Soghomoniam, V.; Chen, Q.; Haushalter, R. C.; Zubieta, J. *Angew. Chem., Int. Ed. Engl.* **1995**, *34*, 223.
(12) Guillou, N.; Gao, Q.; Nogues, M.; Morris, R. E.; Hervieu, M.; Ferey, G.; Cheetham, A. K. *C. R. Acad. Sci. Paris, Ser. 2* **1999**, 387.
(13) Haushalter, R.; Mundi, L. A. *Chem. Mater.* **1992**, *4*, 31.
(14) Zubieta, J. *Comments Inorg. Chem.* **1994**, *16*, 153.
(15) Cavellec, M.; Riou, D.; Greneche, J. M.; Ferey, G. *Inorg. Chem.* **1997**, *36*, 2181.
(16) DeBord, J. R. D.; Reiff, W. M.; Warren, C. J.; Haushalter, R.; Zubieta, J. *Chem. Mater.* **1997**, *9*, 1994.
(17) Lii, K. H.; Huang, Y. F. *J. Chem. Soc., Chem. Commun.* **1997**, 1311.
(18) Zima, V.; Lii, K.-H.; Nguyen, N.; Ducouret, A. *Chem. Mater.* **1998**, *10*, 1914.
(19) DeBord, J.; Reiff, W.; Haushalter, R.; Zubieta, J. *J. Solid State Chem.* **1996**, *125*, 186.
(20) Lii, K.-H.; Huang, Y.-F. *J. Chem. Soc., Dalton Trans.* **1997**, 2221.

10.1021/ic010166g CCC: $20.00
Published on Web 06/02/2001

Table 1. Reagents, Analysis, and Density for the $(C_nH_{2n+6}N_2)[Mn_3(HPO_3)_4]$ ($n = 3-8$) Phases[a]

	analysis									
	mixture of reaction			ICP-AES		C, H, N-elemental analysis			TGA	Density
n	$MnCl_2 \cdot 4H_2O$ (mmol)	H_3PO_3 (mmol)	$C_nH_{2n+4}N_2$ (mmol)	Mn (%)	P (%)	C (%)	H (%)	N (%)	diammonium cation (%)	(g cm^{-3})
3	0.77	3.8	3.8	28.5 (29.4)	21.7 (22.1)	6.2 (6.4)	2.8 (2.9)	5.0 (5.0)	12.8 (13.2)	2.46(2)
4	0.78	3.8	3.9	28.0 (28.7)	21.2 (21.6)	8.2 (8.4)	3.0 (3.2)	4.8 (4.9)	15.3 (15.7)	2.45(2)
5	0.75	7.5	6.0	27.6 (28.0)	20.6 (21.0)	10.1 (10.2)	3.2 (3.4)	4.7 (4.8)	17.5 (17.7)	2.35(2)
6	0.75	7.5	6.2	26.9 (27.3)	20.0 (20.6)	11.7 (12.0)	3.6 (3.7)	4.7 (4.7)	*b*	2.20(1)
7	0.75	7.5	6.2	25.9 (26.7)	19.5 (20.1)	13.3 (13.6)	3.7 (3.9)	4.4 (4.5)	*b*	2.18(2)
8	0.75	7.5	6.2	25.8 (26.1)	19.2 (19.6)	15.0 (15.2)	3.9 (4.2)	4.3 (4.4)	*b*	2.12(5)

[a] The numbers in the parentheses denote the calculated analitical values. The density was measured on single-crystal for the $n = 3$ phase. In the other compounds the measurements were performed on powdered sample as a pellet obtained at 15 Kbar. [b] Superimposed steps.

Table 2. Crystallographic Data for $(C_3H_{12}N_2)[Mn_3(HPO_3)_4]$

chemical formula	$C_3H_{16}N_2O_{12}P_4Mn_3$
a, Å	9.502(1)
b, Å	5.472(1)
c, Å	14.523(4)
β, deg	95.01(3)
V, $Å^3$	752.2(3)
Z	2
fw ($gmol^{-1}$)	560.9
space group	*C* 2/*m* (no. 12)
T, °C	20
radiation, λ(Mo Kα), Å	0.71070
$\rho_{obsd.}$, $\rho_{calcd.}$, g cm^{-3}	2.46(2), 2.476
μ (Mo−Kα), mm^{-1}	2.980
R [$I > 2\sigma(I)$][a]	R1 = 0.026, wR2 = 0.052
R [all data]	R1 = 0.052, wR2 = 0.056

[a] $R1 = [\sum(|F_o| - |F_c|)]/\sum|F_o|$; $wR2 = [\sum[w(|F_o|^2 - |F_c|^2)^2]/\sum[w(|F_o|^2)^2]]^{1/2}$; $w = 1/[\sigma^2|F_o|^2 + (x\ p)^2]$; where $p = [|F_o|^2 + 2|F_c|^2]/3$; $x = 0.0282$.

phosphites have not been studied in a depth way as occurs with the related phosphates. In this way, only four organically templated phosphite compounds with the V(IV), Co(II), and Mn(II) cations are known.[27−29] To explore the possibility of obtaining open-framework metal phosphites, this work was focused on the manganese(II)−alkyldiamine−phosphite acid system. In particular, we present a new series of layered hybrid inorganic−organic manganese(II) phosphites with formula $(C_nH_{2n+6}N_2)[Mn_3(HPO_3)_4]$ ($n = 3-8$), together with the spectroscopic and magnetic properties of the propane-diammonium-manganese(II) phosphite.

Experimental Section

Synthesis and Characterization. The $(C_nH_{2n+6}N_2)[Mn_3(HPO_3)_4]$ ($n = 3-8$) phases were prepared under mild hydrothermal conditions starting from reaction mixtures of $MnCl_2 \cdot 4H_2O$, H_3PO_3 and the corresponding alkyldiamine in a volume of 30 mL of water:butanol (1:2) for $n = 3$ and 4 or water:ethanol (1:1) for $n = 5-8$. The mixtures were stirred up to homogeneity. After that, they were sealed in a PTFE-lined stainless steel pressure vessels (fill factor 75%) and heated at 170 °C for 5 days, followed by slow cooling to room temperature. The pH of the mixtures did not show any appreciable change during the hydrothermal reaction and remained at ca. 7.0. The amount of the chemical reagents used in the synthesis and the percentage of the elements in the products obtained by inductively coupled plasma atomic emission spectroscopy (ICP-AES) together with C, H, N-elemental analysis are presented in Table 1. The density of the products measured by flotation in mixtures of $CHCl_3/CHBr_3$ is also given in Table 1. Well formed light-pink single crystals appeared in the case of the propanediammonium-compound. However, the other phases ($n = 4-8$) were obtained as light pink polycristalline samples.

Thermogravimetric analysis of compounds was carried out under oxygen atmosphere in a SDC 2960 Simultaneous DSC-TGA TA Instrument. Crucibles containing ca. 20 mg of sample were heated at 5 °C min^{-1} in the temperature range 30−800 °C. The results are given in Table 1. The decomposition curves of the $(C_nH_{2n+6}N_2)[Mn_3(HPO_3)_4]$ ($n = 3-5$) compounds reveal a weight loss between ca. 340 and 390 °C, which corresponds to the calcination of the alkyldiammonium cation and agrees well with the calculated values, given in parentheses in Table 1. Between ca. 400 to 800 °C the oxidation process of the phosphite anion occurs without additional weight losses. The thermal decomposition of the alkyldiammonium cation in the $(C_nH_{2n+6}N_2)$ $[Mn_3(HPO_3)_4]$ ($n = 6-8$) phases starts at ca. 340 °C and takes place at the same time as the oxidation process. The X-ray diffraction patterns of the residues obtained from the thermogravimetric analysis at 800 °C show in all the cases the simultaneous presence of $Mn_2P_2O_7$ [*C*2/*m* space group with $a = 6.63(1)$, $b = 8.58(1)$, $c = 4.55(1)$ Å and $\beta = 102.7(1)°$] and $Mn_2P_4O_{12}$ [*C*2/*c* space group with $a = 11.88(1)$, $b = 8.59(1)$, $c = 10.14(1)$ Å and $\beta = 119.2(1)°$].[30]

The thermal behavior of $(C_3H_{12}N_2)[Mn_3(HPO_3)_4]$ was also studied by using time-resolved X-ray thermodiffractometry in air atmosphere. A PHILIPS X′PERT automatic diffractometer (Cu Kα radiation) equipped with a variable-temperature stage (Paar Physica TCU2000) with a Pt sample holder was used in the experiment. The powder patterns were recorded in 2θ steps of 0.02 ° in the range $4 \le 2\theta \le 60°$, counting for 1 s per step and increasing the temperature at 5 °C.min^{-1} from room temperature up to 600 °C. The compound is stable up to ca. 340 °C and the intensity of the monitored (001) peak remains practically unchanged. At around 360 °C, a strong decrease of the (001) peak intensity takes place (ca. 75% of the initial intensity) starting the decomposition of the compound. Between 400 and 500 °C no peaks were observed in the patterns. At temperatures higher than ca. 540 °C peaks belonging to the $Mn_2P_2O_7$ and $Mn_2P_4O_{12}$ phases are observed, in good agreement with the thermogravimetric data. These results indicate that the loss of the propanediammonium cation gives rise to the collapse of the layered architecture and forms condensed manganese(II) phosphates.

Single-Crystal X-ray Diffraction. A prismatic single-crystal of $(C_3H_{12}N_2)[Mn_3(HPO_3)_4]$ with dimensions 0.12 × 0.10 × 0.03 mm was

(21) Chen, J.; Jones, R. H.; Natarajan, S.; Hursthouse, M. B., Thomas, J. M. *Angew. Chem., Int. Ed. Engl.* **1994**, *33*, 639.
(22) DeBord, J.; Haushalter, R.; Zubieta, J. *J. Solid State Chem.* **1996**, *125*, 270.
(23) Cowley, A. R.; Chippindale, A. M. *J. Chem. Soc., Dalton Trans.* **1999**, 2147.
(24) Escobal, J.; Pizarro, J. L.; Mesa, J. L.; Arriortua, M. I.; Rojo, T. *J. Solid State Chem.* **2000**, *154*, 460.
(25) Escobal, J.; Pizarro, J. L.; Mesa, J. L.; Lezama, L.; Olazcuaga, R.; Arriortua, M. I.; Rojo, T. *Chem. Mater.* **2000**, *12*, 376.
(26) (a) Sapiña, F.; Gomez, P.; Marcos, M. D.; Amoros, P.; Ibañez, R.; Beltran, D. *Eur. J. Solid State Inorg. Chem.* **1989**, *26*, 603. (b) Marcos, M. D.; Amoros, P.; Beltran, A.; Martinez, R.; Attfield, J. P. *Chem. Mater.* **1993**, *5*, 121. (c) Attfield, M. P.; Morris, R. E.; Cheetham, A. K. *Acta Crystallogr.* **1994**, *C50*, 981. (d) Marcos, M. D.; Amoros, P.; Le Bail, A. *J. Solid State Chem.* **1993**, *107*, 250.
(27) Bonavia, G.; DeBord, J.; Haushalter, R. C.; Rose, D.; Zubieta, J. *Chem. Mater.* **1995**, *7*, 1995.
(28) Fernandez, S.; Pizarro, J. L.; Mesa, J. L.; Lezama, L.; Arriortua, M. I.; Rojo, T. *Int. J. Inorg. Mater*, in press.
(29) Fernandez, S.; Mesa, J. L.; Pizarro, J. L.; Lezama, L.; Arriortua, M. I.; Olazcuaga, R.; Rojo, T. *Chem. Mater.* **2000**, *12*, 2092.
(30) Powder Diffraction File: Inorganic and Organic, ICDD, Files No. 77-1244 and 38-314, Pennsylvania, USA, 1995.

Table 3. Selected Bond Distances (Å) and Angles (deg) for $(C_3H_{12}N_2)[Mn_3(HPO_3)_4]$ (e.s.d. in Parentheses)

bond distances (Å)			
$Mn(1)O_6$ octahedron		$Mn(2)O_6$ octahedron	
$Mn(1)-O(1)^{i,ii,iii,iv}$	2.222(3)	$Mn(2)-O(1)^{i,iv}$	2.300(3)
$Mn(1)-O(2)^{i,ii}$	2.229(3)	$Mn(2)-O(2)^{i}$	2.293(3)
		$Mn(2)-O(3)^{i}$	2.100(4)
		$Mn(2)-O(4)^{i,iv}$	2.116(3)
$HP(1)O_3$ tetrahedron		$HP(2)O_3$ tetrahedron	
$P(1)-O(1)^{i,v}$	1.525(2)	$P(2)-O(3)^{i}$	1.513(4)
$P(1)-O(2)^{vi}$	1.528(3)	$P(2)-O(4)^{viii,ix}$	1.515(3)
$P(1)-H(1)^{vii}$	1.39(4)	$P(2)-H(2)^{vii}$	1.29(4)
$(H_3N(CH_2)_2NH_3)^{2+}$		$Mn(1)-Mn(2)^{i,ii}$	3.001(1)
$N(1)-C(1)$	1.497(8)		
$C(1)-C(2)$	1.528(9)		
bond angles (deg)			
$Mn(1)O_6$ octahedron		$Mn(2)O_6$ octahedron	
$O(1)^{i}-Mn(1)-O(1)^{iii}$	97.67(9)	$O(1)^{i}-Mn(2)-O(2)^{i}$	79.3(1)
$O(1)^{i}-Mn(1)-O(1)^{iv}$	82.32(9)	$O(1)^{i}-Mn(2)-O(3)^{i}$	94.4(1)
$O(1)^{i}-Mn(1)-O(2)^{i}$	82.36(9)	$O(1)^{i}-Mn(2)-O(4)^{i}$	95.65(9)
$O(1)^{i}-Mn(1)-O(2)^{ii}$	97.64(9)	$O(1)^{i}-Mn(2)-O(1)^{iv}$	78.99(9)
$O(1)^{ii}-Mn(1)-O(1)^{iii}$	82.32(9)	$O(4)^{iv}-Mn(2)-O(1)^{iv}$	95.65(9)
$O(1)^{ii}-Mn(1)-O(1)^{iv}$	97.67(9)	$O(4)^{iv}-Mn(2)-O(2)^{i}$	95.4(1)
$O(1)^{ii}-Mn(1)-O(2)^{i}$	97.64(9)	$O(4)^{iv}-Mn(2)-O(3)^{i}$	90.4(1)
$O(1)^{ii}-Mn(1)-O(2)^{ii}$	82.36(9)	$O(4)^{iv}-Mn(2)-O(4)^{i}$	89.3(1)
$O(2)^{i}-Mn(1)-O(1)^{iii}$	97.64(9)	$O(2)^{i}-Mn(2)-O(1)^{iv}$	79.3(1)
$O(2)^{i}-Mn(1)-O(1)^{iv}$	82.36(9)	$O(2)^{i}-Mn(2)-O(4)^{i}$	95.4(1)
$O(1)^{iii}-Mn(1)-O(2)^{ii}$	82.36(9)	$O(3)^{i}-Mn(2)-O(1)^{iv}$	94.4(1)
$O(1)^{iv}-Mn(1)-O(2)^{ii}$	97.64(9)	$O(3)^{i}-Mn(2)-O(4)^{i}$	90.4(1)
$O(1)^{i}-Mn(1)-O(1)^{ii}$	180.0(4)	$O(1)^{i}-Mn(2)-O(4)^{iv}$	173.1(1)
$O(2)^{i}-Mn(1)-O(2)^{ii}$	180.0(4)	$O(2)^{i}-Mn(2)-O(3)^{i}$	171.8(1)
$O(1)^{iii}-Mn(1)-O(1)^{iv}$	180.0(3)	$O(4)^{i}-Mn(2)-O(1)^{iv}$	173.1(1)
$HP(1)O_3$ tetrahedron		$HP(2)O_3$ tetrahedron	
$O(1)^{i}-P(1)-O(1)^{v}$	113.2(1)	$O(3)^{i}-P(2)-O(4)^{viii}$	110.7(1)
$O(1)^{i}-P(1)-O(2)^{vi}$	113.4(1)	$O(3)^{i}-P(2)-O(4)^{ix}$	110.7(1)
$O(1)^{v}-P(1)-O(2)^{vi}$	113.4(1)	$O(4)^{viii}-P(2)-O(4)^{ix}$	110.9(2)
$O(1)^{i}-P(1)-H(1)^{vii}$	105(1)	$O(3)^{i}-P(2)-H(2)^{vii}$	109(2)
$O(1)^{v}-P(1)-H(1)^{vii}$	105(1)	$O(4)^{viii}-P(2)-H(2)^{vii}$	107(1)
$O(2)^{vi}-P(1)-H(1)^{vii}$	106(1)	$O(4)^{ix}-P(2)-H(2)^{vii}$	107(1)
$(H_3N(CH_2)_2NH_3)^{2+}$			
$N(1)-C(1)-C(2)$	111.2(5)		
$C(1)-C(2)-C(1)^{x}$	110.6(7)		

symmetry codes

$i = x, y, z$	$ii = -x, -y, -z$	$iii = -x, y, -z$	$iv = x, -y, z$
$v = x, -y-1, z$	$vi = x-1/2, y-1/2, z$	$vii = -x-1/2, -y-1/2, -z$	$viii = x-1/2, y+1/2, z$
$ix = x-1/2, -y-1/2, z$	$x = -x+1, y, -z+1$	$xi = x+1/2, y+1/2, z$	$xii = x+1/2, y-1/2, z$
$xiii = x+1/2, -y-1/2, z$			

used for the data collection performed on a STOE IPDS (Imaging Plate Diffraction System) automated diffractometer using graphite-monochromated Mo Kα radiation. The total number of measured reflections was 2687, 783 reflections being independent ($R_{int} = 0.04$) and 547 observed applying the criterion $I > 2\sigma(I)$. Correction for Lorentz and polarization effects were done[31] and also for absorption taking into account the crystal shape by using the XRED program.[32] The structure was solved by direct methods (SHELXS 97).[33] The metal ions and the phosphorus and the oxygen atoms were first located. The nitrogen, carbon, and hydrogen atoms were found in difference Fourier maps, with the exception of the hydrogen atoms belonging to the propanediammonium cation, which were not calculated due to the disorder observed for the carbon atoms. The structure was refined by the full-matrix least-squares method based on F^2, using the SHELXL 97 computer program.[34] The scattering factors were taken from ref 35. All non-hydrogen atoms were assigned anisotropic thermal parameters. The final R factors were R1 = 0.026 [wR2 = 0.052]. Maximum and minimum peaks in final difference synthesis were 0.422 and −0.576 eÅ^{-3}. All drawings were made using ATOMS program.[36] Crystallographic data and selected bond distances and angles are listed in Table 2 and Table 3, respectively.

Physical Techniques. The XRPD patterns were recordered with a PHILIPS X′PERT automatic diffractometer. The IR spectra (KBr pellets) were obtained with a Nicolet FT-IR 740 spectrophotometer in the 400−4000 cm^{-1} range. The Raman spectra were recordered in the 200−3000 cm^{-1} range, with a Nicolet 950FT spectrophotometer equipped with a neodymium laser emitting at 1064 nm. Luminescence measurements were carried out in a Spectrofluorometer Fluorolog-2 SPEX 1680, model F212I at 6.0 K. The excitation source was a high-pressure Xenon lamp emitting between 200 and 1200 nm. The diffuse reflectance spectrum was registered at room temperature on a Cary 2415 spectrometer in the 210−2000 nm range. A Bruker ESP 300 spectrometer was used to record the ESR polycrystalline spectra. The temperature was stabilized by an Oxford Instrument (ITC 4) regulator. The magnetic field was measured with a Bruker BNM 200 gaussmeter and the frequency inside the cavity was determined using a Hewlett-Packard 5352B microwave frequency counter. Magnetic measurements on powdered sample were performed in the temperature range 4.2−300 K, using a Quantum Design MPMS-7 SQUID magnetometer. The magnetic field was approximately 0.1 T, a value in the range of linear dependence of magnetization vs magnetic field even at 4.2 K.

(31) *Stoe IPDS Software*, Version 2.87; Stoe & Cie: Darmstadt, Germany, 1998.
(32) *XRED*; Stoe & Cie GmbH: Darmstadt, Germay, 1998.
(33) Sheldrick, G. M. *SHELXS 97: Program for the Solution of Crystal Structures*; University of Göttingen: Germany, 1997.
(34) Sheldrick, G. M. *SHELXL 97: Program for the Refinement of Crystal Structures*; University of Göttingen: Germany, 1997.
(35) *International Tables for X-ray Crystallography*; Kynoch Press: Birmingham, England; Vol. IV, p 99, 1974.
(36) Dowty, E. *ATOMS: A Computer Program for Displaying Atomic Structures*; Shape Software: Kingsport, TN, 1993.

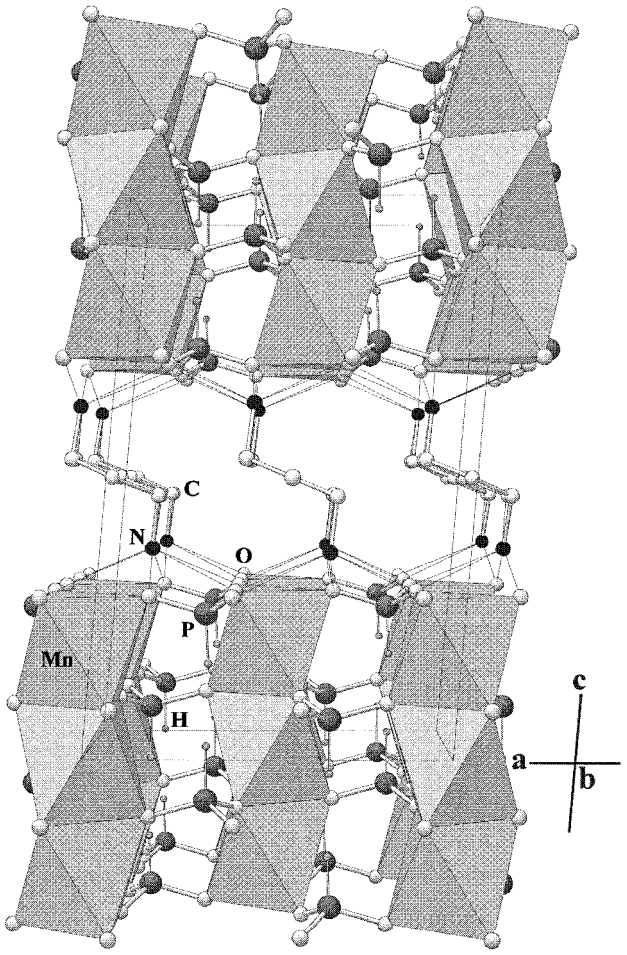

Figure 1. Polyhedral view of $(C_3H_{12}N_2)[Mn_3(HPO_3)_4]$, showing the layered structure.

Results and Discussion

Crystal Structure of $(C_3H_{12}N_2)[Mn_3(HPO_3)_4]$. The $(C_3H_{12}N_2)$-$[Mn_3(HPO_3)_4]$ compound exhibits a layered structure formed by anionic sheets of formula $[Mn_3(HPO_3)_4]^{2-}$, which are extended along the *ab*-plane. The propanediammonium cations are located between the layers existing both ionic interactions and hydrogen bonds with the anionic sheets (Figure 1). This layered architecture has been also found in the related $(C_2H_{10}N_2)$-$[Mn_3(HPO_3)_4]$ phosphite, crystallizing this phase in the triclinic $P\bar{1}$ space group.[29]

The structure of the $[Mn_3(HPO_3)_4]^{2-}$ inorganic sheets can be described as a hexagonal close packing of oxygen atoms (Figure 2). In the layers there is a third of vacancies in the oxygen positions being every oxygen atom surrounded only by four neighbor oxygens in the same layer. The Mn(II) ions occupy a fourth of the interstitial octahedral sites. The phosphorus atoms are located on the interstitial tetrahedral sites delimited by three oxygen atoms belonging to a layer and a vacancy from an internal sheet. The hydrogen of the $(HPO_3)^{2-}$ phosphite anions and the nitrogens of the propanediammonium cations point toward the vacancies on the internal and external sheets, respectively. This result is similar to that observed for the ethylenediammonium phase but the layers are tilted ca. 6° with respect to the *c*-axis.

The Mn(II) ions in the $(C_3H_{12}N_2)[Mn_3(HPO_3)_4]$ phase are hexacoordinated through the oxygen atoms of the phosphite anions. There are two different crystallographic positions for the manganese ions, with 2/*m* and *m* symmetries for Mn(1) and Mn(2), respectively. The MnO_6 octahedra are face-sharing and give rise to a trimeric Mn_3O_{12} unit, with Mn···Mn distance of 3.00(1) Å. These trimeric clusters are bonded to six neighbor trimer entities through the oxygen atoms of the phosphite anions forming layers stacked along the *c*-axis, as was observed in the ethylenediammonium phase. It is worth mentioning that a different feature between both phases is the existence in the propanediammonium compound of a symmetry plane perpendicular to the $[Mn_3(HPO_3)_4]^{2-}$ layers (Figure 3). The absence of this plane in the ethylenediammonium compound determines that the Mn_3O_{12} units are rotated with respect to the *c*-axis (see Figure 3) as was mentioned before.

In the $(C_3H_{12}N_2)[Mn_3(HPO_3)_4]$ compound the $Mn(1)O_6$ octahedra belonging to the Mn_3O_{12} trimer cluster are formed by Mn(1) ions bonded to the $O(1)^{i}$, $O(1)^{ii}$, $O(1)^{iii}$, $O(1)^{iv}$, and $O(2)^{i}$, $O(2)^{ii}$ oxygen atoms from the $HP(1)O_3$ tetrahedra (Figure 4). The mean Mn(1)−O bond distance is 2.224(5) Å similar to that found in the $(C_2H_{10}N_2)[Mn_3\ (HPO_3)_4]$ phase, 2.20(7) Å.[29] In the $Mn(2)O_6$ octahedra the Mn(2) ion is bonded to the $O(3)^{i}$ and $O(4)^{i,iv}$ oxygen atoms from the $HP(2)O_3$ tetrahedra, being the other positions of the coordination sphere occupied by the $O(1)^{i,iv}$ and $O(2)^{i}$ atoms of the $HP(1)O_3$ tetrahedra. The mean bond length is 2.2(1) Å. The *cis*- and *trans*-O−Mn−O angles in the MnO_6 octahedra indicate a topology near to octahedral

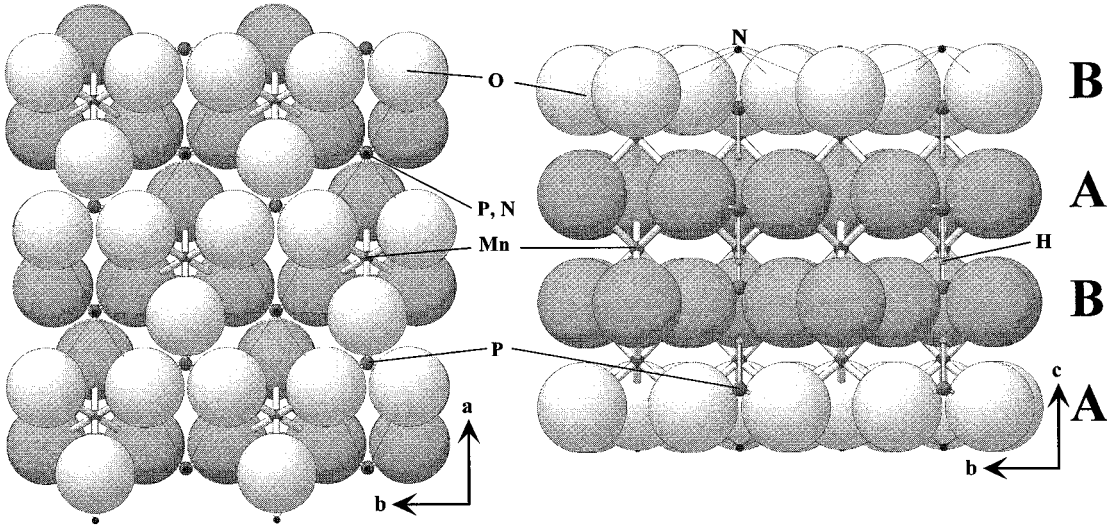

Figure 2. Hexagonal close packing of the $[Mn_3(HPO_3)_4]^{2-}$ sheets.

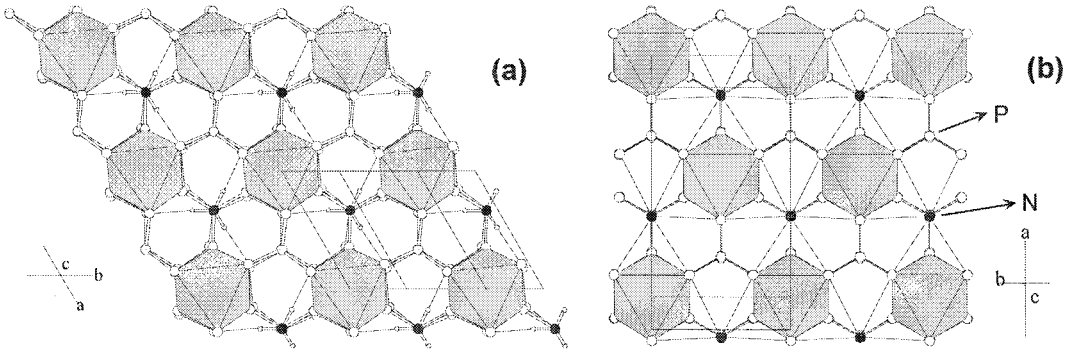

Figure 3. Projection on the (001) plane of the $[Mn_3(HPO_3)_4]^{2-}$ sheets, belonging to the (a) $(C_2H_{10}N_2)[Mn_3(HPO_3)_4]$ and (b) $(C_3H_{12}N_2)[Mn_3(HPO_3)_4]$ compounds.

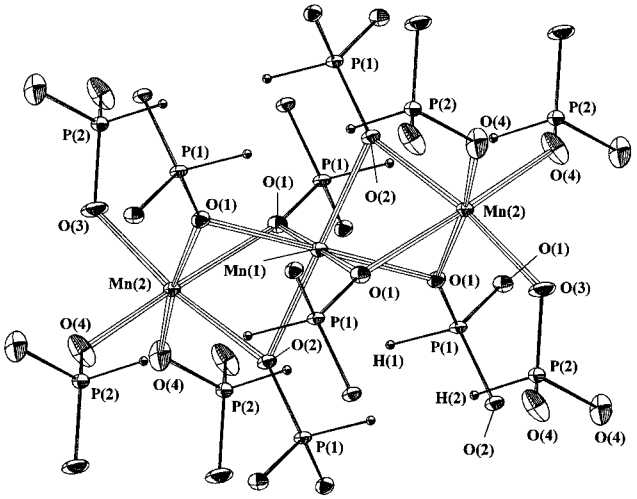

Figure 4. ORTEP drawing (50% thermal ellipsoids) of the Mn_3O_{12} cluster of $(C_3H_{12}N_2)[Mn_3(HPO_3)_4]$ with detailed labeling of the atoms.

(see Table 3). The Mn−O−Mn angles in the Mn_3O_{12} unit of $(C_3H_{12}N_2)[Mn_3(HPO_3)_4]$ are 83.12(8) and 83.1(1)° for the Mn(1)−O(1)−Mn(2) and Mn(1)−O(2)−Mn(2), respectively, similar to those found in the $(C_2H_{10}N_2)[Mn_3(HPO_3)_4]$ phase.[29] In both compounds the Mn(2)−Mn(1)−Mn(2) angle is 180°.

In the HPO_3 tetrahedra, the P−O and H−P bonds exhibit a mean value of 1.520(7) and 1.34(7) Å, respectively. The O−P−O and H−P−O angles show values usually found in the tetrahedral coordination. The propane-diammonium cation exhibits disorder in the position of the carbon atoms with occupancy factors of 50%, giving rise to two different possible orientations for this cation with respect to the 2/*m* symmetry elements (Scheme 1). The C−C and C−N bond distances and angles are in the range usually found for this cation.[37] The C−N fragment is placed practically perpendicular to the $[Mn_3(HPO_3)_4]^{2-}$ layers, being the N(1) atom near to six different oxygen atoms of the $HP(2)O_3$ anion (see Scheme 1). The bond lengths for the hydrogen bonds are as follows: $N(1)\cdots O(3)^{xi,xii}$−P(2), 2.963(2) Å; $N(1)\cdots O(4)^{i,iv}$−P(2), 2.931(5) Å; and $N(1)\cdots O(4)^{xi,xiii}$−P(2), 2.968(5) Å. Scheme 1 shows the existence of two possibilities for the hydrogen bonds between the propanediammonium cation and the phosphite anion. However, the positions of the oxygen atoms involved in these hydrogen contacts are unknown because the hydrogen atomic coordinates of the propanediammonium cation were not found.

X-ray Powder Diffraction Study of the $(C_nH_{2n+6}N_2)$ $[Mn_3(HPO_3)_4]$ (n = 3−8) Alkyldiammonium Compounds. The

Scheme 1

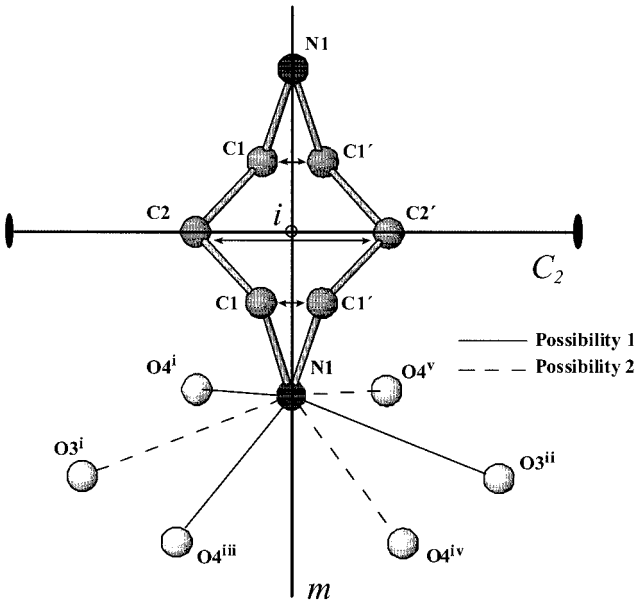

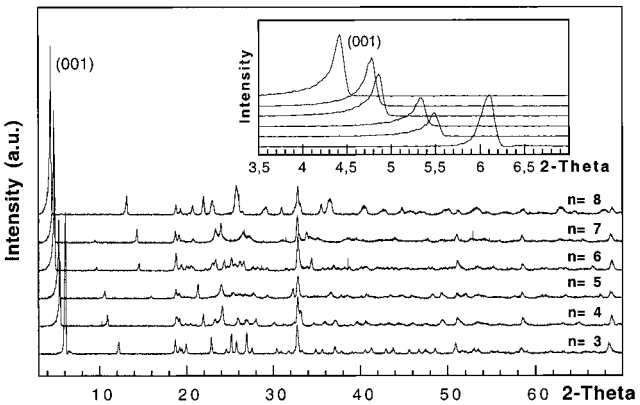

Figure 5. X-ray powder diffraction patterns of the $(C_nH_{2n+6}N_2)[Mn_3(HPO_3)_4]$ (n = 3−8) phases.

XRPD patterns of the $(C_nH_{2n+6}N_2)[Mn_3(HPO_3)_4]$ (n = 3−8) phases are shown in Figure 5. They have been refined with the Rietveld method (pattern matching routine)[38] using, as the starting model, the unit cell parameters and the space group of $(C_3H_{12}N_2)[Mn_3(HPO_3)_4]$, which were obtained from single-crystal data. The lattice parameters obtained from the Rietveld refinement are given in Table 4. In the diffractograms the (001)

(37) Gharbi, A.; Jouini, A.; Averbuch-Pouchot, M. T.; Durif, A. *J. Solid State Chem.* **1994**, *111*, 330.

(38) Rodriguez-Carvajal, J. *FULLPROF, Program Rietveld Pattern Matching Analysis of Powder Patterns*; Grenoble: Illinois, 1994, unpublished.

Table 4. Lattice Parameters for the $(C_nH_{2n+6}N_2)[Mn_3(HPO_3)_4]$ ($n = 4-8$) Phases

compound (n)	a (Å)	b (Å)	c (Å)	β (deg)	Vol (Å^3)
4	9.468(2)	5.478(3)	16.246(4)	94.4(1)	840.3(3)
5	9.463(1)	5.471(1)	16.740(2)	95.9(1)	862.0(2)
6	9.454(2)	5.465(1)	18.383(3)	96.3(1)	944.0(3)
7	9.475(2)	5.610(1)	18.552(3)	91.5(1)	985.8(3)
8	9.455(1)	5.455(1)	20.242(2)	90.8(1)	1044.0(2)

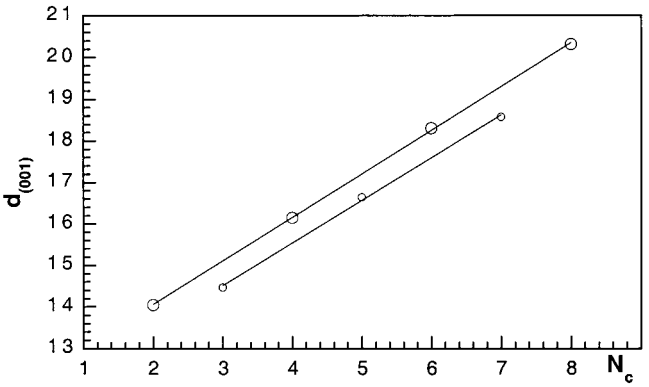

Figure 6. d_{001} interlayer distance vs carbon number of intercalated alkyldiammoium cations in the $(C_nH_{2n+6}N_2)[Mn_3(HPO_3)_4]$ ($n = 2-8$) series. The d_{001} value for the $n = 2$ phase was taken from ref 29.

reflection exhibits a stronger intensity than that observed for the other peaks (see Figure 5). This fact is characteristic of layered compounds. Furthermore, the (001) reflection is shifted to lower 2θ-values when the number of the carbon atoms increases in the $(C_nH_{2n+6}N_2)[Mn_3(HPO_3)_4]$ series (see inset in Figure 5). This shift is related to the interlayer distances. The relationship between the basal spacing (d_{001}) and the number of carbon atoms in the diammonium cation (N_c) is shown in Figure 6. These data can be described by the following expressions:

$$d_{001} = 11.965 + 1.0485\, N_c$$

$$d_{001} = 11.429 + 1.0275\, N_c$$

for N_c-values even or odd, respectively.

The mean increase of the basal spacings per carbon atom, $\Delta d_{001}/\Delta N_c$, in these compounds is 1.05 or 1.03 for N_c-values even or odd, respectively. The increase of alkyl chain length per carbon atom is 1.27 Å for a straight trans−trans alkylamine.[39] So, the mean increase per carbon atom observed in these compounds involves that the alkyldiammonium chains must be tilted with respect to the $[Mn_3(HPO_3)_4]^{2-}$ layers at angles of 55.6° or 54.0°, for chains with N_c-values even or odd, respectively. These angles agree well with those found for other layered hydrogen phosphates,[40] such as 58.7° in α-$Ti(HPO_4)_2 \cdot H_2O$, 54.2° in α-$Zr(HPO_4)_2 \cdot H_2O$, 66° in α-$Sn(HPO_4)_2 \cdot H_2O$, 59.6° in $VOHPO_4 \cdot 0.5H_2O$, and 53.2° in $HNiPO_4 \cdot H_2O$[41] and also with the theoretical tilt angle of 53.8° for the alkylamines in which the C−N bond is nearly perpendicular to the basal plane.[40] The arrangement of the organic cation suggests that more than one H-bond may be stablished between the $-(NH_3)^+$ groups and the layer-surface oxygen atoms of the $(C_nH_{2n+6}N_2)[Mn_3(HPO_3)_4]$ compounds, as was observed in the ethylene-[29] and propane-diammonium compounds from single-crystal data. So, we can conclude that in the $(C_nH_{2n+6}N_2)[Mn_3(HPO_3)_4]$ compounds with N_c being even the alkyldiammonium cation adopts the arrangement shown in Figure 7a, with the C−N bond perpendicular to the $[Mn_3(HPO_3)_4]^{2-}$ sheets and the C-atoms of the alkyldiammonium cation in trans form, being the tilt angle with respect to the inorganic layers of ca. 56°. The arrangement of the C−N bonds determines that for the alkyldiammonium cations with N_c being odd, one C-atom cannot adopt the trans form being, in this case, the tilt angle of the organic cation of ca. 54° (Figure 7b). This fact could be the responsible of the disorder observed for the carbon atoms of the propanediammonium cation in the crystal structure of $(C_3H_{12}N_2)[Mn_3(HPO_3)_4]$.

Infrared and Raman Spectroscopies of the $(C_nH_{2n+6}N_2)[Mn_3(HPO_3)_4]$ ($n = 3-8$) Phases. The Infrared and Raman spectra of the $(C_nH_{2n+6}N_2)[Mn_3(HPO_3)_4]$ ($n = 3-8$) phases show the same features. The spectra exhibit in all cases the bands corresponding to the vibrations of the alkyldiammonium cations and phosphite $(HPO_3)^{2-}$ anions. Selected bands obtained from both IR and Raman spectra are given in Table 5, as average values for all the studied compounds. The results are similar to those found in the literature for other alkyldiammonium phases.[37,42−44]

Luminescence and UV−Vis Spectroscopies of $(C_3H_{12}N_2)[Mn_3(HPO_3)_4]$. The emission spectrum of $(C_3H_{12}N_2)[Mn_3(HPO_3)_4]$ obtained at 6.0 K under a 365 nm excitation is shown in the inset of Figure 8. The spectrum is characteristic of an octahedral environment for the Mn(II) (d^5) ions with a unique red emission peaking at 650 nm. The excitation spectrum ($\lambda_{em} = 660$ nm) (Figure 8) reveals the spectral distribution of bands corresponding to the excited levels of Mn(II) in octahedral environment [$^4T_1(^4G)$, 551 nm; $^4T_2(^4G)$, 446 nm; $^4A_1,^4E(^4G)$, 406 nm; $^4T_2(^4D)$, 366 nm; $^4E(^4D)$, 342 nm].[45,46] Furthermore, the diffuse reflectance spectrum exhibits very weak spin-forbidden d−d bands at ca. 335, 350, 405, 435, and 535 nm, as characteristic of Mn(II) d^5 high spin cation in octahedral symmetry. The Dq parameter is 880 cm^{-1} and the Racah, B and C, parameters are 660 and 3610 cm^{-1}, respectively. These values correspond with those usually found for octahedrally coordinated Mn(II) compounds.[25,29,47−49] The B-value is ca. 69% of that corresponding to the free Mn(II) ion (960 cm^{-1}) which indicates a significant degree of covalence in the Mn−O bonds.

ESR and Magnetic Properties of $(C_3H_{12}N_2)[Mn_3(HPO_3)_4]$. The X-band ESR spectra of $(C_3H_{12}N_2)[Mn_3(HPO_3)_4]$ were recorded on powdered sample at room temperature and 7 K (Figure 9). The spectra show isotropic signals with a "g"-value of 2.008 which remains unchanged with variation in temperature. This result agrees with an octahedral coordination for the Mn(II) ions as was found from the structural data. The line width and the intensity of the spectra show temperature dependence. The intensity decreases with decreasing temperature whereas the line width increases from 36.5 up to 102.5 mT when the

(39) Lagaly, G. *Solid State Ionics* **1986**, *22*, 43.
(40) Gulianst, V. V.; Benzinger, J. B.; Sundaresan, S. *Chem. Mater.* **1994**, *6*, 353.
(41) Goñi, A.; Rius, J.; Insausti, M.; Lezama, L.; Pizarro, J. L.; Arriortua, M. I.; Rojo, T. *Chem. Mater.* **1996**, *8*, 1052.
(42) Dolphin, D.; Wick, A. E. *Tabulation of Infrared Spectral Data*; John Wiley & Sons: New York, 1977.
(43) Tsuboi, M. *J. Am. Chem. Soc.* **1957**, *79*, 1351.
(44) Nakamoto, K. *Infrared and Raman Spectra of Inorganic and Coordination Compounds*; John Wiley & Sons: New York, 1997.
(45) Orgel, L. E. *J. Chem. Phys.* **1955**, *23*, 1004.
(46) Tanabe, Y.; Sugano, S. *J. Phys. Soc. Jpn.* **1954**, *9*, 753.
(47) Lever, A. B. P. *Inorganic Electronic Spectroscopy*; Elsevier Science Publishers B. V.: Amsterdam, Netherlands, 1984.
(48) Lawson, K. E. *J. Chem. Phys.* **1966**, *44*, 4159.
(49) Escobal, J.; Mesa, J. L.; Pizarro, J. L.; Lezama, L.; Olazcuaga, R.; Rojo, T. *J. Mater. Chem.* **1999**, *9*, 2691.

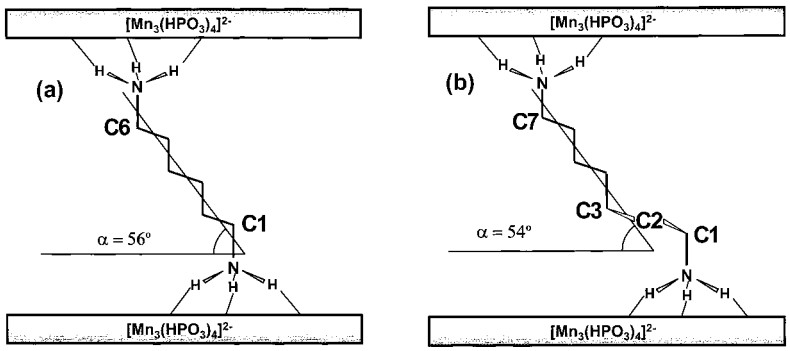

Figure 7. Model proposed for the disposition of the alkyldiammonium cations inside the interlayer space of the $(C_nH_{2n+6}N_2)[Mn_3(HPO_3)_4]$ phases, (a) *n* being even; (b) *n* being odd.

Table 5. Selected Bands (average values in cm^{-1}) from the IR and Raman Spectra for the $(C_nH_{2n+6}N_2)[Mn_3(HPO_3)_4]$ ($n = 3-8$) Phases[a]

assignment	IR	Raman
$\nu(-NH_3)^+$	3120 (w)	
$\nu(-CH_2-)$	2975−2555 (m)	2975−2870 (w)
ν(HP)	2475, 2435 (m)	2475, 2435 (s)
$\delta(NH_3)^+$	1580 (m)	1560 (w)
$\delta(-CH_2-)$	1525−1465 (w)	1465−1340 (w)
$\nu_{as}(PO_3)$	1105, 1085 (m,s)	1075, 1055 (w,m)
δ(HP)	1035, 990 (s,m)	1025, 1010 (m,s)
$\nu_s(PO_3)$	920 (m)	990 (m)
$\delta_s(PO_3)$	640, 610 (m)	650, 605 (w)
$\delta_{as}(PO_3)$	490, 455 (m,w)	485, 450 (w)

[a] ν = stretching; δ = deformation; s = symmetric; as = asymmetric; w = weak; m = medium; s = strong.

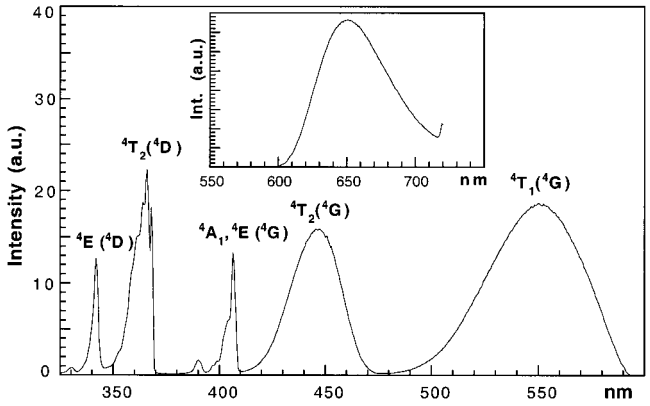

Figure 8. Emission spectrum ($\lambda_{exc} = 365$ nm), inset, and excitation spectrum ($\lambda_{em} = 660$ nm) of $(C_3H_{12}N_2)[Mn_3(HPO_3)_4]$ at 6.0 K.

temperature ranges from 293 to 7 K, probably due to a strong spin correlation.[50−54]

Magnetic measurements of $(C_3H_{12}N_2)[Mn_3(HPO_3)_4]$ were performed on a powdered sample from 4.2 to 300 K. The molar magnetic susceptibility increases with decreasing temperature in the range studied and the $\chi_m T$ product decreases from 10.95 cm^3K/mol at 300 K to 0.93 cm^3K/mol at 4.2 K (Figure 10). These results indicate the existence of antiferromagnetic interactions.

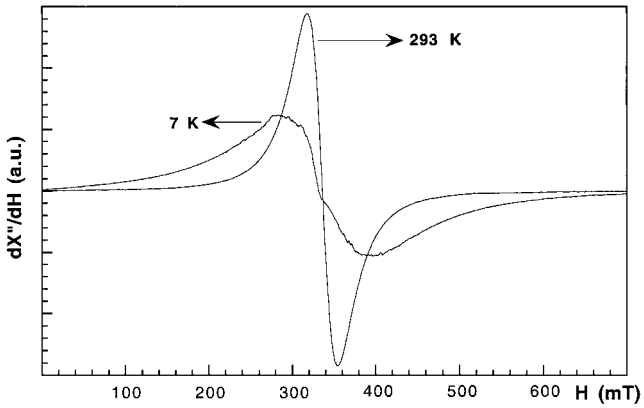

Figure 9. Powder X-band ESR spectra of $(C_3H_{12}N_2)[Mn_3(HPO_3)_4]$, at 293 and 7 K.

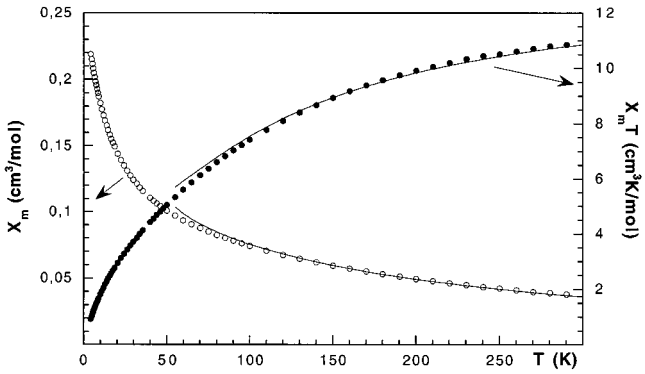

Figure 10. Thermal evolution of χ_m and $\chi_m T$ curves of $(C_3H_{12}N_2)[Mn_3(HPO_3)_4]$. The solid lines show the fit of the χ_m and $\chi_m T$ experimental data to a model for isolated trimers.

Taking into account that in the crystal structure the interlayer distance is ca. 14 Å and the absence of any maximum in the χ_m vs *T* curve we can disregard a three-dimensional model in the analysis of the magnetic data. Furthermore, considering the existence of sheets formed by linear trimer units, the Van Vleck expression for the susceptibility of a trimer with non interaction between the extreme ions could be a priori used for the magnetic study of this compound,[55]

$$\chi = [Ng^2\beta^2/3kT][u/u']$$

where $u = \sum_{S_{13},S} S(S+1)(2S+1)\exp(-E(S_{13},S)/kT)$ and $u' = \sum_{S_{13},S}(2S+1)\exp(-E(S_{13},S)/kT)$. The results obtained in the fit (solid lines in Figure 10) indicate that only the magnetic data above ca. 90 K can be reasonably fitted to the above

(50) Wijn, H. W.; Walker, L. R.; Daris, J. L.; Guggenheim, H. *J. Solid Sate Commun.* **1972**, *11*, 803.
(51) Richards, P. M.; Salamon, M. B. *Phys. Rev. B* **1974**, *9*, 32.
(52) Escuer, A.; Vicente, R.; Goher, M. A. S.; Mautner, F. *Inorg. Chem.* **1995**, *34*, 5707.
(53) Bencini, A.; Gatteschi, D. *EPR of Exchange Coupled Systems*; Springer-Verlag: Berlin, 1990.
(54) Cheung, T. T. P.; Soos, Z. G.; Dietz, R. E.; Merrit, F. R. *Phys. Rev. B* **1978**, *17*, 1266.
(55) Kahn, O. *Molecular Magnetism*; VCH Publishers: New York, 1993.

expression, with a value of the *J*-exchange parameter of $J = -15$ K and $g = 2.008$ (from the ESR spectra). If we consider the existence of magnetic interactions between neighbor trimers connected via phosphite anions, in the form of a *J′*-parameter in the expression of the magnetic susceptibility, the fit does not show a substantial improvement. So, we can conclude that at high temperatures this system could be considered as formed by isolated linear trimers, but at temperatures lower than 90 K a long magnetic ordering must be established, giving rise to a more complex system in which the magnetic interactions propagated via phosphite anions inside the layers are predominant in the compound. This hypothesis seems to be supported by the value of 0.93 cm^3K/mol found for the χ_mT product at 4.2 K, instead of the value of 4.37 cm^3K/mol expected for an uncoupled Mn(II) ion with $S = {}^5/_2$ and $g = 2.0$.

The χ_mT values observed for the propanediammonium phase are slightly higher than those obtained for the ethylenediammonium compound (10.48 and 0.87 cm^3K/mol, at room temperature and 4.2 K, respectively).[29] These results together with the estimated *J*-exchange parameters indicate the presence of slightly smaller antiferromagnetic interactions in the propanediammonium compound. This fact could be attributed to the presence of slight differences in the bond angles implicated in the exchange interaction pathways corresponding to these alkyldiammonium phases, as was observed from the crystallographic data.

The magnetic exchange inside the Mn_3O_{12} trimer clusters of these compounds can take place through *(i)* the oxygen atoms of the phosphite anions which link the sharing faces MnO_6 octahedra; the mean values of the O−Mn−O angles are of ca. 83° and 84°, in the propane- and ethylene-diammonium compounds, respectively, and could give rise to ferromagnetic interactions, *(ii)* a direct intratrimeric interaction involving the $d_{x^2-y^2}$ and d_{xz} orbitals of the Mn(II) ions at ca. 3.0 Å. The dihedral angle between the MnO_4 equatorial planes is of ca. 121° and 119°, for the propane- and ethylene-diammonium compounds, respectively, which should lead to antiferromagnetic couplings. These exchange pathways inside the trimer units, together with the intertrimeric interactions propagated through the oxygen atoms of the phosphite anions in the *ab*-plane, determine the antiferromagnetic overall behavior observed for the $(C_2H_{10}N_2)$ $[Mn_3(HPO_3)_4]$ and $(C_3H_{12}N_2)[Mn_3(HPO_3)_4]$ compounds.

Concluding Remarks

A new series of layered inorganic−organic hybrid manganese(II) phosphites with the formula $(C_nH_{2n+6}N_2)[Mn_3(HPO_3)_4]$ ($n = 3-8$) has been synthesized by using mild hydrothermal conditions. The $(C_3H_{12}N_2)$ $[Mn_3(HPO_3)_4]$ phase was obtained in the form of single crystals whereas the other compounds were prepared as powdered samples. The crystal structure of the propanediammonium compound consists of sheets with composition $[Mn_3(HPO_3)_4]^{2-}$, stacked along the *c*-axis and with the alkyldiammonium cation placed between the layers. These layers are constructed from face-sharing MnO_6 octahedra which give rise to trimeric Mn_3O_{12} entities interconnected by $(HPO_3)^{2-}$ phosphite anions in the *ab*-plane. The analysis of the X-ray powder diffraction patterns of the $(C_nH_{2n+6}N_2)[Mn_3(HPO_3)_4]$ ($n = 4-8$) phases indicates that they are isotypes with the propanediammonium compound. The tilt angle of the lineal alkyldiammonium cation with respect to the inorganic $[Mn_3(HPO_3)_4]^{2-}$ sheets is ca. 55° allowing to the organic cations the formation of three hydrogen bonds with the oxygen atoms of the phosphite anions. This fact favors the layered structure of these compounds. The thermogravimetric analysis of $(C_3H_{12}N_2)$-$[Mn_3(HPO_3)_4]$ shows that the crystal structure collapses after the loss of the propanediammonium cation. The values calculated for the Dq and Racah parameters in the $(C_3H_{12}N_2)[Mn_3(HPO_3)_4]$ phase agrees with the existence of Mn(II) ions in an octahedral symmetry. The magnetic behavior indicates the presence of antiferromagnetic interactions inside the trimer units of $(C_3H_{12}N_2)[Mn_3(HPO_3)_4]$, which at low temperatures are also propagated along the $[Mn_3(HPO_3)_4]^{2-}$ sheets via phosphite anions.

Acknowledgment. This work was financially supported by the Ministerio de Educación y Ciencia and Universidad del País Vasco/EHU (Grants PB97-0640 and 169.310-EB149/98), which we gratefully acknowledge. We thank F. Guillen and E. Marquestaut (I.C.M.C.B., Pessac, France) for luminescence and ESR measurements at low temperature and Dpto. Física de la Materia Condensada of the UPV/EHU for use of the STOE IPDS automatic diffractometer. S. Fernandez thanks the Gobierno Vasco/Eusko Jaurlaritza for a doctoral fellowship.

Supporting Information Available: Four X-ray crystallographic files, in CIF format, are available. This material is available free of charge via the Internet at http://pubs.acs.org.

IC010166G